

6BIO Enhances Oligonucleotide Activity in Cells: A Potential Combinatorial Anti-androgen Receptor Therapy in Prostate Cancer Cells

Xiaowei Zhang,¹ Daniela Castanotto,^{1,2} Sangkil Nam,² David Horne,² and Cy Stein^{1,2}

¹Departments of Medical Oncology and Experimental Therapeutics and Molecular and Cellular Biology, City of Hope Medical Center, Duarte, CA 91010, USA; ²Beckman Research Institute, City of Hope Medical Center, Duarte, CA 91010, USA

Approximately 15%–25% of men diagnosed with prostate cancer do not survive their disease. The American Cancer Society estimated that for the year 2016 the number of prostate cancer deaths will be 26,120. Thus, there is a critical need for novel approaches to treat this deadly disease. Using high-throughput small-molecule screening, we found that the small molecule 6-bromo-indirubin-3'-oxime (6BIO) significantly improves the targeting of antisense oligonucleotides (ASOs) delivered by gymnosis (i.e., in the absence of any transfection reagents) in both the cell cytoplasm and the nucleus. Furthermore, as a single agent, 6BIO had the unexpected ability to simultaneously downregulate androgen receptor (AR) expression and AR signaling in prostate cancer cells. This includes downregulating levels of the AR-V7, a drug-resistance-related AR splice variant that is important in the progression of prostate cancer. Combining 6BIO and an anti-AR oligonucleotide (AR-ASO) can augment the downregulation of AR expression. We also demonstrated that 6BIO enhances ASO function and represses AR expression through the inhibition of the two main glycogen synthase kinase 3 (GSK-3) isoforms: GSK-3 α and GSK-3 β activity. Our findings provide a rationale for the use of 6BIO as a single agent or as part of a combinatorial ASO-based therapy in the treatment of human prostate cancer.

INTRODUCTION

Prostate cancer is the second most common cancer in men and one of the leading causes of cancer-related deaths worldwide.¹ The androgen receptor (AR) represents perhaps the most important target in the treatment of this disease. Although patients with prostate cancer initially respond to androgen deprivation therapy, nearly all patients will eventually relapse and progress to castration-resistant prostate cancer (CRPC).² The new generation of anti-AR signaling drugs for CRPC, represented by enzalutamide (an AR inhibitor) and abiraterone (an androgen synthesis inhibitor), has further confirmed that suppression of AR signaling still represents a therapeutic rationale for advanced prostate cancer after therapy with primary androgen deprivation.^{3,4} However, these drugs extend overall survival for only several months on average because of the emergence of drug resistance. One of the potential molecular determinants of disease progression to CRPC, in addition to drug resistance, is the production

of the AR-V7,^{5,6} an AR splice variant that lacks the C-terminal ligand-binding domain and is constitutively active.⁷

Antisense oligonucleotides (ASOs) containing the appropriate chemical modifications and delivered by gymnosis provide the possibility of rational design and represent an attractive targeted strategy for cancer treatment.⁸ Single-stranded ASOs regulate gene expression by induction of nuclease-mediated degradation of their complementary RNA sequences.⁹ Over the past several decades, a variety of nucleotide modifications have been introduced that improve the stability and the biological function of ASOs. These include the phosphorothioate (PS) modification and the incorporation of locked nucleic acids (LNAs) (referred to as LNA gapmers if the LNAs are incorporated at the 3' and 5' molecular termini, or LNA mixmers if the LNAs appear also at internal sites)^{10,11} that provide increased nuclease stability and higher T_m without diminishing oligonucleotide (oligo) activity.

The ability of PS oligos to enter the cells without transfection reagents ("free uptake") had been appreciated for several years,¹² but the discovery of gymnosis,^{9,13–16} which demonstrated that these PS LNA oligos can not only enter cells, but can also produce gene silencing, has placed these potentially therapeutic molecules among the leaders in the arsenal of experimental oligos. Absent the side effects of transfection, in vitro gymnotic delivery of ASOs more closely parallels the administration of saline formulations of ASOs in vivo. However, despite years of developmental work, ASOs have progressed slowly in the clinic. There are many reasons for this, but approaches that augment gymnotic delivery, such as use of small molecules,¹⁷ might be useful to maximize the clinical potential of therapeutic ASOs.

Received 20 July 2016; accepted 11 October 2016;
<http://dx.doi.org/10.1016/j.ymthe.2016.10.017>.

Correspondence: Daniela Castanotto, Departments of Medical Oncology and Experimental Therapeutics and Molecular and Cellular Biology and Beckman Research Institute, City of Hope Medical Center, 1500 E. Duarte Rd., Duarte, CA 91010, USA.
E-mail: dcastanotto@coh.org

Correspondence: Cy Stein, Departments of Medical Oncology and Experimental Therapeutics and Molecular and Cellular Biology and Beckman Research Institute, City of Hope Medical Center, 1500 E. Duarte Rd., Duarte, CA 91010, USA.
E-mail: cstein@coh.org

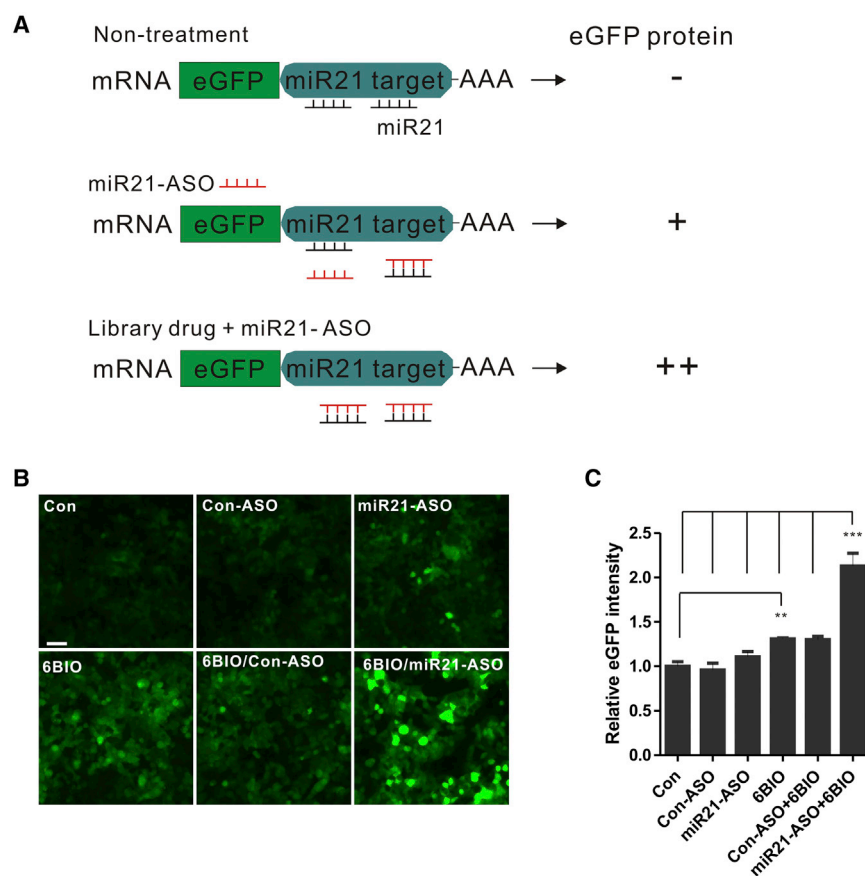


Figure 1. 6BIO Enhances miR21-ASO Function in the Cell Cytoplasm

(A) Schematic representation of the high-throughput screen used to select small molecules that enhance miR21-ASO antagonism activity in HCT116-EGFP-miR21 cells. The HCT116 cells express an EGFP transcript containing multiple miR21 targeting sites in its 3' UTR. The miR21-ASO binds to and blocks the function of the complementary endogenous mature miR21 sequence, thus restoring EGFP expression. Micrographs (B) and EGFP signal intensity (C) of HCT116-EGFP-miR21 cells treated with miR21-ASO alone or in combination with 1 μ M 6BIO. Ten thousand cells were cultured in clear-bottom, black 96-well plates and treated with or without 1 μ M 6BIO and 1 μ M miR21-ASO for 3 days. The EGFP fluorescence intensity was read by a microplate reader as described in the [Materials and Methods](#). Scale bar, 50 μ M. Data are expressed as the mean \pm SD. n = 3. **p < 0.01 (Student's t-test); ***p < 0.001.

RESULTS

6BIO Enhances miR21-ASO Function in the Cell Cytoplasm

We performed a high-throughput screen of several small-molecular chemical libraries using the HCT116-EGFP-miR21 cell system²⁷ to identify small molecules that increase the uptake and/or activity of ASOs delivered by gymnosin. These cells stably express an EGFP

mRNA containing multiple microRNA-21 (miR21) targeting sites within its 3' UTR.^{27,28} The binding of the endogenous miR21 to these sites blocks translation and prevents EGFP expression (Figure 1A). EGFP expression can be reinstated via a miR21 antagonism,²⁹ which specifically binds to the mature miR21 sequence and releases the translational block. Therefore, the amount of EGFP expression in this system is a reflection of antagonism activity. To perform our screen, we used an miR21-ASO; this is an anti-miR21 PS LNA mixmer oligo complementary to the mature miR21 sequence. LNA PS mixmers contain LNA modifications at the 3' and 5' molecular termini and are interspersed at internal sites, thus masking RNase H activity. The results of the high-throughput screen identified the indirubin derivative 6BIO (Figure S1) as the most potent enhancer of miR21-ASO function. HCT116-EGFP-miR21 cells treated with the combination of the miR21-ASO and 6BIO (6BIO/miR21-ASO; Figures 1B and 1C) demonstrated significantly increased EGFP expression (approximately 2-fold, n = 3, p < 0.001) when compared with the miR21-ASO alone (Figures 1B and 1C, miR21-ASO). Surprisingly, treatment with 6BIO alone (Figures 1B and 1C, 6BIO) increased the EGFP signal by approximately 30% (n = 3, p < 0.001), perhaps because of an inhibitory effect on endogenous miR21 expression.³⁰

To investigate whether 6BIO could also improve ASO function in more complex microenvironments that might be more similar to

ASOs offer an approach to selectively target the AR. Anti-AR oligos (AR-ASOs) have recently been developed that effectively repress AR expression at both the mRNA and the protein level in preclinical prostate cancer models.^{18,19} However, a phase 1 study of a PS LNA gapmer anti-AR-ASO in patients with advanced prostate cancer demonstrated only a limited number of PSA responses and significant dose-related toxicity.²⁰ In this study, we discovered that the small molecule 6-bromo-indirubin-3'-oxime (6BIO), an anti-leukemia indirubin derivative,²¹ possesses multiple anti-prostate cancer activities. 6BIO has been reported to regulate cellular viability, proliferation, and apoptosis and act as an anti-tumor agent in a variety of human cancer models, including melanoma,²² breast cancer,²³ bladder cancer,²⁴ and lymphoma.²⁵ 6BIO has been found to suppress the lung metastasis of an aggressive breast cancer through inhibiting cell adhesion, migration, and invasion.²⁶ Strikingly, we found that it also represses both the AR and the AR-V7 gene expression as a single agent, and it enhances AR-ASO function when the ASO is delivered by gymnosin to prostate cancer cells. To our knowledge, there is no therapeutic agent currently available that can effectively repress the AR-V7 splice variant. Furthermore, the combinatorial use of 6BIO and an AR-targeted oligo greatly increased AR targeting. This can potentially result in the use of reduced drug doses and in the reduction of toxicity.

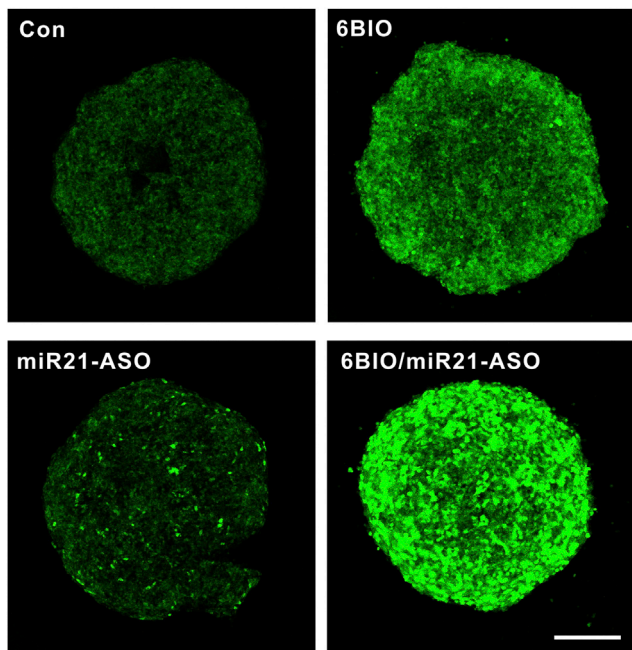


Figure 2. 6BIO Enhances miR21-ASO Function in Tumor Microspheroids

A total of 20,000 HCT116-EGFP-miR21 cells in 40 μ L complete media were loaded into each well of a 96-well hanging drop culture plate, as described in the [Materials and Methods](#). After 24 hr, 1 μ M 6BIO (6BIO, top row) and/or 1 μ M miR21-ASO (6BIO/miR21-ASO or miR21-ASO, bottom row) in 10 μ L complete media were added to the formed microspheres. After 3 additional days, the treated microspheres were harvested for two-photon confocal microscopy. DMSO, which is used to dissolve 6BIO, was used as the negative control (Con). Scale bar, 500 μ M.

those found in actual tumors, we examined 3D cultures of HCT116-EGFP-miR21 cells.³¹ 6BIO aided the penetration of the miR21-ASO into the 3D tumor microspheroids and strikingly increased EGFP expression by enhancing the block of the endogenous miR21 ([Figure 2](#), compare miR21-ASO versus 6BIO/miR21-ASO). Because miRNAs are processed in the cytoplasm, which is also the site where the EGFP translational block occurs, 6BIO enhancement of miR21-ASO in 2D cell cultures, as well as in tumor microspheroids, indicates that the compound likely improves ASO antagonism function in the cytoplasm.

6BIO Enhances Splice-Switching Oligo Function in the Cell Nucleus

Unlike liposome-mediated ASO delivery, which can lead to extensive ASO loading in the nucleus,³² gymnotic delivery of ASOs results in bulk ASO accumulation predominately in the cytoplasm, with much smaller amounts of oligo being transported into the nucleus.^{16,33} To investigate whether 6BIO could facilitate the ability of ASOs delivered by gymnotic to modulate molecular events that occur solely in the nucleus, we used a splice-switching oligo (SSO) targeted to the EGFP pre-mRNA.^{17,34} This system relies on cells (HeLa-EGFP-654) stably expressing an EGFP pre-mRNA whose coding sequence has been interrupted by the insertion of an additional exon.^{17,34}

The binding of an SSO to the first 3' splice site causes the skipping of this internal exon and restores the correct EGFP reading frame and EGFP protein expression.^{17,34} Thus, the resulting EGFP expression is a direct reflection of the potency of the SSO. To trigger exon skipping, we used an LNA PS mixmer with the identical LNA distribution as we used for the miR21 antagonism screen.

In our experiments, the SSO, but not the non-targeting mixmer control oligo (Con-ASO), redirected splicing and restored EGFP expression ([Figure 3A](#), top row, compare SSO versus Con-ASO). Consistent with the results we obtained using the miR21 antagonism, the combination of the SSO with 6BIO noticeably increased (approximately 65%) EGFP expression ([Figure 3A](#), compare SSO, top row, with SSO/6BIO, bottom row). Quantitative flow cytometric assays examining the effect of 6BIO on SSO activity ([Figures 3B and 3C](#)) confirmed that 6BIO treatment (SSO+6BIO) enhanced the ability of the SSO to induce splice switching. This is demonstrated by a more than 3-fold increase ($n = 3$, $p < 0.001$) in the number of EGFP-positive cells compared with SSO treatment alone ([Figures 3B and 3C](#)). Neither the non-targeting control oligo (Con-ASO) nor 6BIO alone (6BIO), nor a combination of the two (Con-ASO+6BIO), produced any effect on EGFP expression ([Figures 3B and 3C](#)). This indicates that 6BIO increases pre-mRNA exon skipping in the cell nucleus through the enhancement of SSO activity.

6BIO Activity Extends to ASOs that Target Oncogenes in Prostate Cancer Cells

We evaluated 6BIO to determine whether it affected the activity of other potentially therapeutic LNA-PS ASO gapmers, including an anti-AR ASO, in prostate cancer cells. In contrast with mixmers, which are internally modified oligos, gapmers contain LNA modifications only at the 3' and 5' molecular termini. These oligos rely on RNase H activity to silence their RNA targets. Unexpectedly, 1 μ M 6BIO alone repressed AR mRNA expression in LNCaP cells ([Figure 4A](#), 6BIO). However, the combined treatment of 6BIO and an AR-ASO resulted in the greatest suppression, producing a >60% reduction ($n = 3$, $p < 0.001$) in androgen receptor mRNA expression ([Figure 4A](#), AR-ASO+6BIO). Although the AR-ASO alone did not cause mRNA reduction at the time chosen for the analysis (48 h; [Figure 4A](#), AR-ASO), the expression of the AR protein was still somewhat reduced ([Figures 4D, 5C \[LNCaP\], and 5D \[LAPC-4\]](#)). This discrepancy in protein and mRNA levels has been previously observed³³ and may be because of the binding of the oligo to the AR mRNA coupled with a subsequent translational block.

These data were confirmed with titration experiments using the AR-ASO or 6BIO ([Figures 5A and 5B](#)). The combined treatment of 6BIO (1 μ M) and the AR-ASO (2 μ M) reduced AR protein expression approximately 70%, compared with a 24% reduction when the AR-ASO alone was used ([Figure 5A](#)) and 26% when 6BIO alone was used ([Figure 5A](#)). Significantly lower concentrations of 6BIO (0.25 and 0.5 μ M) and the AR-ASO (1 μ M) were still able to produce >60% suppression of AR protein expression at 0.25 μ M 6BIO, and nearly 90% suppression at 0.5 μ M 6BIO ([Figure 5C](#), 0.25 6BIO

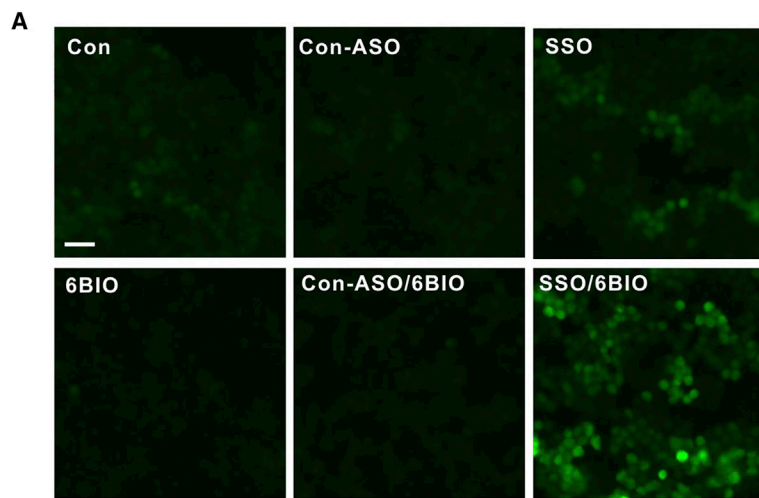
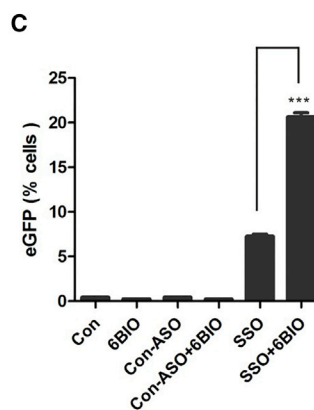
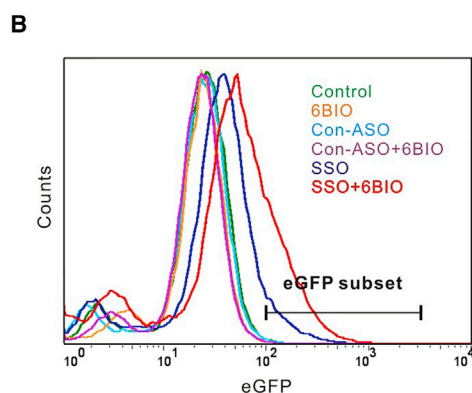


Figure 3. 6BIO Enhances SSO Function in the Cell Nucleus

(A) Photomicrographs of HeLa-EGFP-654 cells treated with DMSO control (Con), 1 μ M non-targeting oligo (Con-ASO), 1 μ M SSO (SSO), 2 μ M 6BIO (6BIO), a combination of 1 μ M control oligo and 2 μ M 6BIO (Con-ASO/6BIO) or 1 μ M SSO and 2 μ M 6BIO (SSO/6BIO) as indicated, for 2 days prior to imaging. Scale bar, 50 μ M. (B) Representative experiment showing the analysis of flow cytometric data obtained from HeLa-EGFP-654 cells treated as in (A). The EGFP subset gate was defined by defining the non-treated control cells as EGFP-negative. The profiles shown are typical of several independent experiments. (C) The graph represents the combined flow cytometric data analysis of three different experiments. The y axis indicates the percentage of cells in the EGFP subset window. Data are expressed as the mean \pm SD. $n = 3$. *** $p < 0.001$ (Student's t test).



for the fraction inhibition (F_a) = 0.50–0.90, indicative of robust synergy.³⁶

A similar outcome was observed when we targeted three additional oncogenes: β -catenin (Figures 4B and 4E), BCL2 (Figures 4C and 4F), and HER3 (data not shown).^{16,37,38} The effects of the combination of 6BIO and the ASO on the targeting on β -catenin were of particular interest in view of the potential capability of 6BIO to activate the Wnt/ β -catenin pathway³⁹ through the suppression of glycogen synthase kinase (GSK)-3 β , a β -catenin inhibitor.³⁹ Nevertheless, the treatment of LNCaP cells with 6BIO and a β -catenin ASO (β -Cat-ASO+

[AR-ASO 1 μ M +] and 0.5 6BIO [AR-ASO 1 μ M +]). Approximately 5-fold more AR-ASO (5 versus 1 μ M) was required to achieve about a 50% suppression of the AR protein expression when used without the addition of 6BIO (Figure 5B, AR-ASO 5.0 6BIO –). Higher concentrations of 6BIO alone (up to 5 μ M) reduced AR expression by a maximum of 56%. However, the combination of 5 μ M 6BIO with 1 μ M AR-ASO nearly eliminated the AR protein expression (Figure 5C, 5.0 6BIO [AR-ASO 1 μ M +]). This effect on AR inhibition could also be demonstrated in LAPC-4 cells (Figure 5D). To quantify the interaction between the two drug treatments, we performed a detailed dose-response analysis and generated a combination index (CI) plot using the Chou-Talalay method³⁵ (Figure 5E; Figure S2). The straight line (CI = 1; Figure 5E) represents the additive effect of the drugs analyzed. A CI > 1 or a CI < 1 demonstrates antagonism or synergism, respectively, between two or more drugs given in combination. All the points, which were calculated by quantification of the western blots (of which one example is shown in Figure S2), fall below CI = 1 (Figure 5E). Therefore, the combination of 6BIO and the AR-ASO demonstrates synergistic suppression of the AR. The value of the CI ranged between 0.37 and 0.30

6BIO) still decreased the β -catenin mRNA expression by approximately 90% compared with a 65% reduction with ASO alone (Figure 4B, compare β -Cat-ASO+6BIO with β -Cat-ASO; $n = 3$; $p < 0.001$). The mRNA expression data under the conditions of our experiment were congruent with the protein expression data (a reduction of 92%; β -Cat-ASO+6BIO versus 63% β -Cat-ASO; Figure 4E). The combined treatment with 6BIO and a BCL2-ASO generated an approximately 75% decrease in BCL2 mRNA expression, whereas treatment with oligo alone reduced BCL2 mRNA expression by only 38% (Figure 4C, compare BCL2-ASO+6BIO versus BCL2-ASO; $n = 3$; $p < 0.01$). Here, too, the levels of protein expression, under the conditions of the experiment, were congruent with the mRNA expression results (84% BCL2-ASO+6BIO versus 40% BCL2-ASO; Figure 4F). In addition, the reduction of HER3 expression was approximately 62% with the combined treatment and 28% with HER3-ASO alone ($n = 3$; $p < 0.001$; data not shown).

In contrast with what we observed for the AR mRNA and protein, which are downregulated by 6BIO alone (Figures 4A and 4D), BCL2 mRNA and protein expression showed an approximate

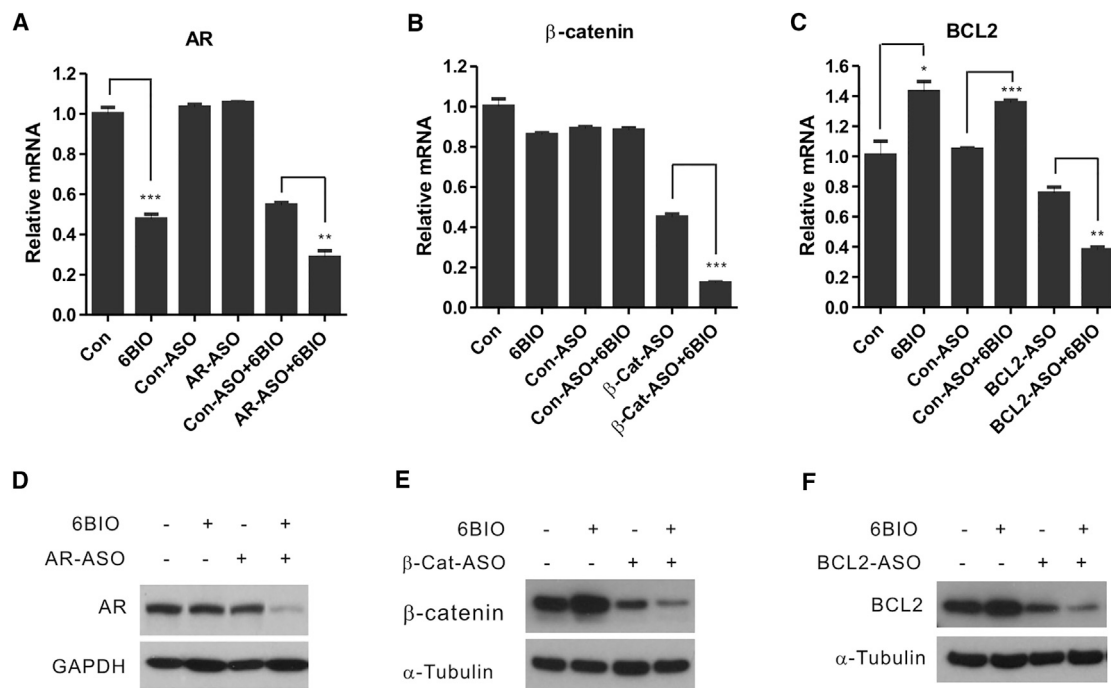


Figure 4. 6BIO Enhances the Activity of PS LNA Gapmers Delivered by Gymnosis in Prostate Cancer Cells

(A–C) RT-PCR detection of ASO-targeted gene expression in LNCaP cells treated for 2 days with (A) 1 μ M AR-ASO, (B) 5 μ M β -Cat-ASO, or (C) 1 μ M BCL2-ASO, with or without 1 μ M 6BIO. Values were normalized to β -actin mRNA expression and expressed as the mean \pm SD. $n = 3$. * $p < 0.05$, ** $p < 0.01$, *** $p < 0.001$, Student's t test. The graphs show the residual mRNA expression values subsequent to the indicated treatments. (D–F) Representative western blot analyses of AR, β -catenin, and BCL2 protein expression in LNCaP cells treated for 3 days with (D) 1 μ M AR-ASO, (E) 1 μ M β -Cat-ASO, or (F) 1 μ M BCL2-ASO, with (+) or without (–) 1 μ M 6BIO. Values of protein reduction were calculated with ImageJ and normalized to α -tubulin or GAPDH as loading controls and to the control, untreated cells. The experiments were repeated a minimum of two times with similar results.

30% increase after treatment ($n = 3$, $p < 0.05$; Figures 4C and 4F). Treatment with 6BIO alone also consistently increased β -catenin protein expression, but not mRNA levels, by approximately 20% (Figures 4B and 4E). This is likely due to the inhibition of GSK-3 β activity by 6BIO.⁴⁰ GSK-3 β is known to phosphorylate the β -catenin protein and to enhance its degradation.⁴¹ Blocking the activity of GSK-3 β will thus elevate levels of β -catenin.⁴² However, in every case, 6BIO was able to enhance oligo-directed downregulation of the targeted mRNAs. It should be noted that 6BIO did not enhance the uptake of a Cy5-labeled PS LNA gapmer ASO in LNCaP cells, as determined by flow cytometry (Figure S3). Taken together, these data indicate that 6BIO enhances the function of potentially therapeutic ASOs in prostate cancer cells.

6BIO Suppresses AR and AR Signaling in Prostate Cancer Cells

The finding that in LNCaP cells 6BIO significantly downregulated AR mRNA expression (Figure 4A) and protein levels (Figures 4D and 5A–5D) prompted us to further investigate its effects in other cell lines and on AR signaling. Pharmacologically relevant concentrations of 6BIO significantly repressed mRNA (Figures 6A–6C) and protein (Figures 6D–6I) levels of the AR gene in all three prostate cell lines analyzed; LNCaP (which express a mutant full-length AR; Figures 6A and 6D, AR), LAPC-4 (which express a wild-type full-length

AR; Figures 6B and 6E, AR), and 22Rv1 (which express a wild-type full-length AR and exons 4–8 deleted AR-V7 isoform; Figures 6C and 6F, AR and AR-V7). The inhibitory effect of 6BIO on AR expression was dose- (Figures 6D–6F) and time-dependent (Figures 6G–6I), and it could be detected at concentrations as low as 0.1 μ M (Figure S4). Importantly, 6BIO also significantly inhibited the expression of the AR-V7 (Figures 6C and 6F; Figure S4B), an AR-splice variant that is constitutively located in the nucleus and continuously activates the expression of cell survival genes.^{5,6} Strikingly, 4–5 μ M 6BIO was sufficient to completely abrogate protein expression of the wild-type AR and the AR-V7 isoform (Figures 6F and 6I). Consistent with the decrease in AR protein expression, 6BIO significantly repressed AR signaling in these three cell lines, as exemplified by the reduction in the levels of *PSA* and *TMRPSS3* mRNA expression (Figures 6A–6C; Figure S4), which are downstream of the AR.

6BIO Inhibits Prostate Cancer Cell Growth

The finding that 6BIO induced BCL2 expression (Figures 4C and 4F), coupled with its ability to activate the Wnt/ β -catenin pathway, most likely by preventing β -catenin protein degradation (Figure 4E), makes 6BIO an attractive AR-targeting agent. We therefore examined the effects of 6BIO on the growth of prostate cancer cells in tissue culture.

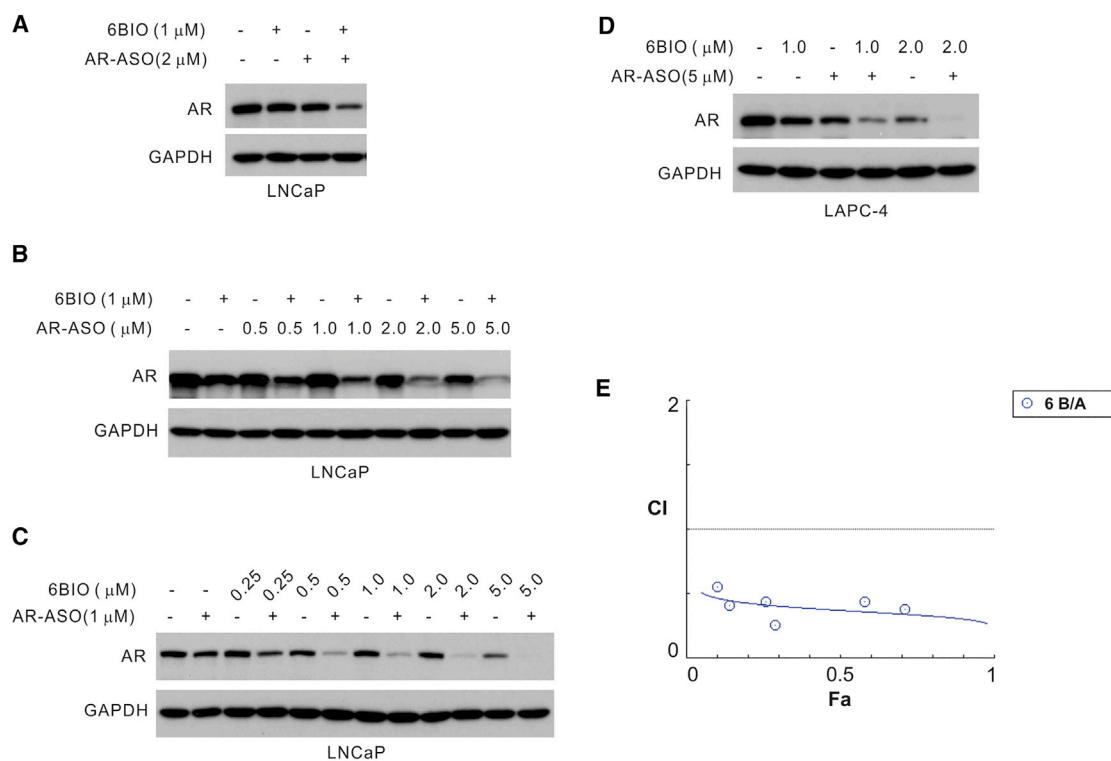


Figure 5. Titration Experiments Using the AR-ASO and 6BIO Demonstrate a Reduced AR Expression in Prostate Cancer Cells

Western analyses of lysates harvested from LNCaP (A–C) or LAPC-4 cells (D). (A) LNCaP cells treated with (+) or without (–) 1 μ M 6BIO or 2 μ M AR-ASO. The combined treatment of 6BIO and the AR-ASO reduced AR protein expression by approximately 70%. Either 6BIO or AR-ASO alone reduced the AR protein expression by only approximately 25%. Values of protein reduction were calculated with ImageJ and normalized to the GAPDH as the loading control and to the control, untreated cells. (B) LNCaP cells treated with 1 μ M 6BIO with (+) or without (–) the indicated concentrations of AR-ASO. (C) LNCaP cells treated with 1 μ M AR-ASO with (+) or without (–) the indicated concentrations of 6BIO. (D) LAPC-4 cells with 5 μ M AR-ASO with (+) or without (–) the indicated concentrations of 6BIO. In all experiments, the AR-ASO was delivered by gymnotus for 2 days. Experiments were repeated a minimum of two times with consistent results. (E) Combination index (CI) plot calculated with the CI equation algorithms using CompuSyn software.³⁵ The values were derived from the quantitation of AR protein suppression by the combined use of 6BIO and AR-ASO (Figure S2). CI = 1 indicates an additive effect of the drugs; CI > 1 indicates an antagonistic effect; CI < 1 demonstrates synergism.

We found that 6BIO induced LNCaP cell growth inhibition in a dose-dependent manner (Figures S5A and S5B). 6BIO concentrations (0.1–2 μ M) slightly increased mitochondrial function, as determined by MTS assays (Figure S5A). However, at an increased concentration, LNCaP cell growth is inhibited (MTS). However, when the cells were counted (Figure S5B), an approximately 20% ($n = 3$) reduction in cell numbers could be seen at a concentration of 1–2 μ M ($p < 0.05$ [1 μ M], $p < 0.001$ [2 μ M]). To simulate *in vivo* prostate cancer growth, we cultured the LNCaP cells in Matrigel. Treatment with low 6BIO concentrations (0.25 μ M) significantly inhibited tumor microsphere formation with respect to both the number (Figure S5C) and the size (Figure S5D) of the individual tumor microspheres. A higher 6BIO concentration (1 μ M) completely inhibited tumor microsphere formation (Figures S5C and S5D).

6BIO Enhances Gymnotic SSO Function and Represses AR Signaling by Inhibiting Both GSK-3 α and GSK-3 β Activity

Among the reported targets of 6BIO is the GSK-3 kinase,^{22,26,40,43–45} which consists of two distinct isoforms, GSK-3 α and GSK-3 β , and

which has been implicated in multiple cellular processes and in prostate cancer pathogenesis.^{46,47} To understand the mechanism of action of 6BIO, we used another GSK-3 α/β inhibitor, CHIR99021, to determine whether it had similar effects as 6BIO on ASO activity and AR regulation. Similar to what was observed with 6BIO (Figures 3A–3C), the combination of increasing concentrations of CHIR99021 with the EGFP-SSO in HeLa-EGFP-654 cells increased SSO activity as determined by EGFP expression, when compared with the SSO alone (Figure 7A, compare SSO-CHIR with SSO). However, this effect was not as potent as the combined treatment of SSO with 6BIO (Figure 7A, compare SSO-CHIR with SSO-6BIO). Similarly, CHIR99021 downregulated the expression of the AR and PSA mRNAs in LNCaP cells to a lesser extent than 6BIO (Figure 7B). Although 6BIO was also more potent on a molar basis, CHIR99021 inhibited AR protein expression (approximately 50% [5 μ M]; Figure 7C) and AR-V7 (nearly total suppression at 10 μ M; Figure 7D) in LNCaP and 22Rv1 cells, respectively. 6BIO was also more potent than lithium chloride (LiCl), also a GSK-3 α/β inhibitor (compare 6BIO 1–2 μ M with LiCl 1 mM [Figure 7C] and 6BIO 4 μ M with LiCl 1 mM [Figure 7D]).

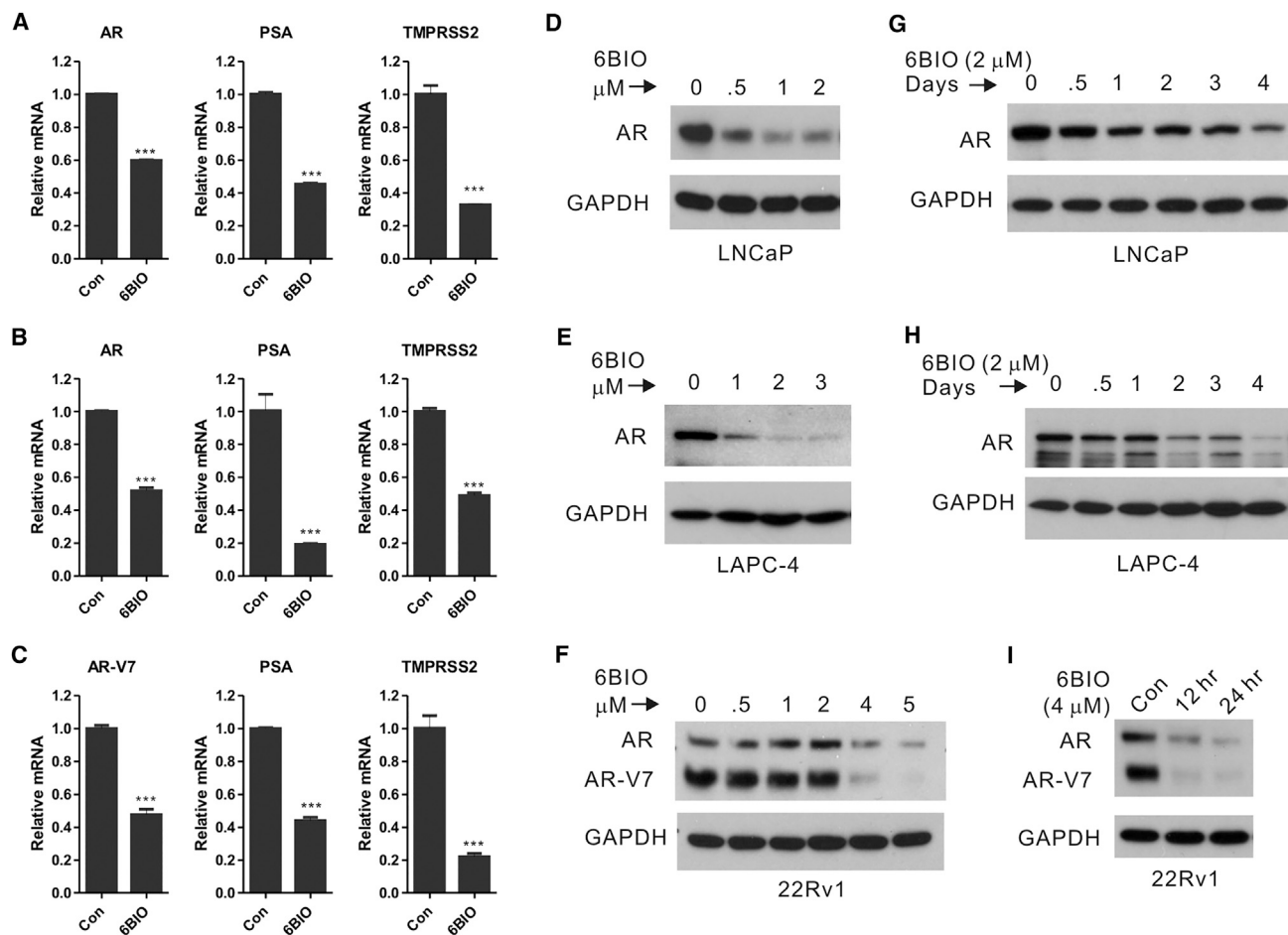


Figure 6. 6BIO Targets the AR and Inhibits AR Signaling in Prostate Cancer Cells

(A–C) Relative AR, PSA, and TMPRSS3 gene expression as determined by RT-PCR from total RNA derived from (A) LNCaP, (B) LAPC-4, and (C) 22Rv1 cells treated with 1 μ M 6BIO for 24 hr. Values were normalized to β -actin mRNA expression and expressed as the mean \pm SD. $n = 3$. *** $p < 0.001$, Student's t test. (D–I) Representative western blot analysis of LNCaP (D and G), LAPC-4 (E and H), and 22Rv1 (F and I) cells treated with increasing concentrations of 6BIO for 2–3 days (D–F) or increasing treatment times at 2 or 4 μ M concentration of 6BIO (G–I), as indicated. Values of protein reduction were calculated with ImageJ and normalized to GAPDH as the loading control and to the control, untreated cells. The experiments were repeated at least twice with similar results. AR, full-length AR; AR-V7, exons 4–8 deleted V7 isoform.

To further characterize the relation between GSK-3 α/β inhibition, AR repression, and the functional role of each GSK-3 isoform, we used small interfering RNAs (siRNAs) to silence GSK-3 α and/or GSK-3 β in prostate cancer cells. Interestingly, the silencing of either the GSK-3 α or the GSK-3 β isoforms did not produce significant downregulation of AR mRNA (compare si- α and si- β with si-Con; Figure 8A, AR) or protein expression (compare si- α and si- β with si-Con; Figure 8B, AR row). However, simultaneous siRNA silencing of GSK-3 α and GSK-3 β with three different siRNAs targeting both isoforms (si- $\alpha\beta$ 1–3) inhibited (up to approximately 50%) AR mRNA (compare si- $\alpha\beta$ 1–3 with si-Con; Figure 8A, AR) and nearly eliminated AR protein expression (compare si- $\alpha\beta$ 1–3 with si-Con; Figure 8B, AR row) in LNCaP cells. The effects of GSK-3 α and GSK-3 β siRNA-mediated silencing on AR protein expression were confirmed in an additional prostate cancer cell line (LAPC-4; Figure 8C). Predictably, silencing of GSK-3 α and GSK-3 β also affected

AR signaling as demonstrated by the reduction in the levels of AR-targeted PSA and TMPRSS3 mRNA expression (Figure 8A, PSA and TMPRSS3, compare si- $\alpha\beta$ 1–3 with si-Con). These results parallel the activity of 6BIO in these cells. Therefore, the data strongly indicate that GSK-3 α and GSK-3 β are the critical targets for 6BIO that lead to AR repression. Furthermore, our data highlight the functional redundancy of these two isoforms with respect to AR regulation in prostate cancer cells.

DISCUSSION

Despite the explosive growth in knowledge about human cancers, effectively targeting the molecular drivers in many types of cancer cells remains an unmet challenge. PS LNA ASOs delivered by gymnosis represent a clinically practical approach for molecularly targeted therapy. However, the slow progress in the therapeutic development of ASOs requires alternative strategies to augment their activity. The

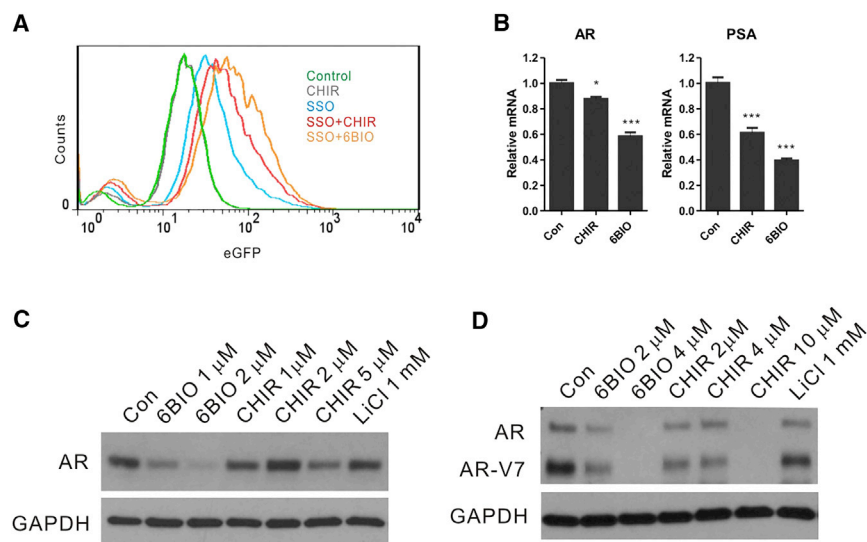


Figure 7. 6BIO Produces Potent Suppression of AR and AR-V7 Expression in Prostate Cancer Cells Compared with Other GSK-3 Inhibitors

(A) Flow cytometric data analysis of EGFP expression in HeLa-EGFP-654 cells treated with 10 μ M CHIR and 2 μ M 6BIO with or without SSO for 2 days. The profiles shown are typical of several independent experiments. (B) RT-PCR analysis of RNA harvested from LNCaP cells treated with 1 μ M CHIR or 1 μ M 6BIO for 24 hr. CHIR represses AR and PSA expression in LNCaP cells, although not to the same extent as 6BIO. Untreated cells (Con) served as the control for these experiments. Values were normalized to β -actin mRNA expression and expressed as the mean \pm SD. $n = 3$. * $p < 0.05$, *** $p < 0.001$, Student's t test. Representative western blot of (C) LNCaP and (D) 22Rv1 cells, treated with the indicated concentrations of 6BIO, CHIR, or lithium chloride (LiCl) for 3 days. In LNCaP cells, a minimum of 5 μ M CHIR is required to achieve a comparable AR suppression as 1 μ M 6BIO. In 22Rv1 cells, 10 μ M CHIR is required to achieve the same full AR suppression as 4 μ M 6BIO. LiCl treatment of both LNCaP and 22Rv1 cells showed little effect on AR downregulation at up to a 1 mM concentration. GAPDH was used as the standard control. The experiments were repeated two times with similar results.

identification of small molecules that facilitate ASO activity is a step in this direction.^{17,48} In this study, we used small-molecule high-throughput screening to identify the kinase inhibitor 6BIO as an enhancer of the activity of potentially therapeutic PS LNA ASOs delivered by gymnosin. Pharmacological concentrations of 6BIO augmented the activity of an ASO targeted to the endogenous oncogenic miR21 in HCT116-miR21 cells (Figures 1 and 2), augmented the activity of a pre-mRNA SSO used to rescue EGFP expression in HeLa-eGFP-654 cells (Figure 3), and augmented conventional RNase H-mediated gapmer ASO gene silencing of BCL2, β -catenin, and HER3 expression in prostate cancer cells (Figure 4 and data not shown). In addition, concentrations of 6BIO as low as 0.1 μ M inhibited AR and AR-V7 mRNA and protein expression, as well as AR signaling in prostate cancer cells (Figures 5, 6, and S4). Importantly, an even higher concentration of 6BIO did not demonstrate significant toxicity in vivo in a melanoma xenograft mice model.²² Moreover, to our knowledge, this is the first time that a small molecule has been shown to silence expression of the AR-V7. Furthermore, we demonstrated that the mechanism of 6BIO's profound repression of AR expression occurs through the simultaneous inhibition of GSK-3 α and GSK-3 β . Remarkably, the combination of 6BIO with a PS LNA AR-ASO virtually eliminated AR expression in prostate cancer cells (Figures 5D and 5D) in culture.

6BIO is a derivative of indirubin, an active component of a traditional Chinese herbal medicine that has been used for treatment of chronic myelogenous leukemia.^{21,23} Indirubin and its derivatives have been reported to function as protein kinase inhibitors by interacting with the kinase ATP-binding pocket.^{23,44,49,50} Numerous studies have also commented on its activity in maintaining the self-renewal and pluripotency of embryonic stem cells through activating the

Wnt/ β -catenin pathway and in promoting the proliferation of cardiomyocytes.^{30,51,52} 6BIO's multiple biological activities can be reflected by the wide spectrum of kinases it inhibits. These include the CDK family members CDK1, CDK2, and CDK5, in addition to PDK1, JAK/STAT3, and GSK-3 α/β .^{22,26,40,43–45}

GSK-3 α/β is a ubiquitously expressed serine-threonine kinase encoded by distinct genes.⁴⁷ The two isoforms share 97% sequence homology within their catalytic domains but differ in their C and N termini.⁴⁷ GSK-3 α/β has been found to be involved in a wide range of cellular processes ranging from glycogen metabolism and cell growth to membrane vesicle trafficking and autophagy.^{53,54} It is a critical regulator of numerous signaling pathways including the insulin and Hedgehog pathways.⁴⁷ The GSK-3 α/β proteins inhibit the Wnt/ β -catenin pathway via their ability to phosphorylate β -catenin. This marks the protein for ubiquitination and degradation. In our experiments, congruent with this activity, 6BIO treatment increased β -catenin protein (Figure 4E), but not RNA (Figure 4B), expression in LNCaP cells, probably by acting as a GSK-3 α/β inhibitor.

6BIO also induced the increased expression of both BCL2 mRNA and protein in LNCaP cells (Figures 4C and 4F). Nuclear factor- κ B (NF- κ B) is a transcriptional regulatory factor of BCL2 in mammalian cells.⁵⁵ A recent study demonstrated an inverse relationship between GSK-3 signaling and NF κ B activity,⁵⁶ which may explain the upregulation of BCL2 expression after GSK-3 inhibition. Despite the fact that 6BIO induced the upregulation of BCL2 and β -catenin proteins, their expression could still be silenced by the combinatorial treatment of 6BIO with a PS LNA gapmer ASO in LNCaP cells (Figures 4E and 4F).

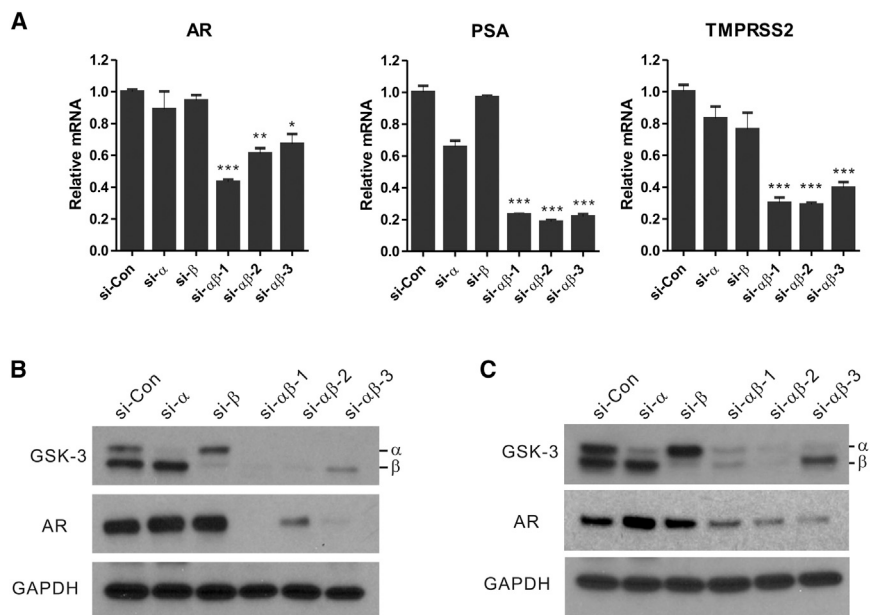


Figure 8. siRNA-Mediated Silencing of GSK-3 α and GSK-3 β Suppresses AR Expression and AR Signaling in Prostate Cancer Cells

(A) The use of different siRNA sequences targeting GSK-3 α (si- α), GSK-3 β (si- β), or both (si- $\alpha\beta$ -1, si- $\alpha\beta$ -2, si- $\alpha\beta$ -3) show that simultaneous targeting of GSK-3 α and GSK-3 β is required for the suppression of AR, PSA, and TMPRSS3 mRNA expression in LNCaP cells. Two days following siRNA transfection, cells were harvested and mRNA levels were determined via quantitative RT-PCR. Values were normalized to β -actin mRNA expression and expressed as the mean \pm SD. $n = 3$. * $p < 0.05$, ** $p < 0.01$, *** $p < 0.001$, Student's t test. LNCaP (B) and LAPC-4 cells (C) were transfected with GSK-3 α , GSK-3 β , or GSK-3 α/β siRNAs as described in (A). Protein expression levels were determined by western blot analysis. si-Con is a non-targeting si-RNA control. Values of protein reduction were calculated by ImageJ and normalized to the GAPDH as the loading control and to the cells treated with the siRNA control. Western blot experiments were repeated three times in LNCaP cells and two times in LAPC-4 cells.

Our understanding of how oligos are transported and function within cells is increasing but still imperfect.^{12,16,33} It is commonly accepted that ASOs delivered by gymnosin are internalized into cells through the process of endocytosis. They then enter the membrane vesicle endosome-lysosome shuttling system. In our experiments, 6BIO exposure for 3 hr did not increase the uptake of a Cy5-labeled PS LNA gapmer BCL2 ASO in LNCaP or HT1080 cells. Prolonged exposure up to 12 hr diminished the accumulation of this Cy5-labeled ASO in LNCaP cells (Figure S3). These results indicate that 6BIO's stimulation of ASO activity occurred subsequent to the initial endocytosis process. The PDK1 and JAK/STAT3 signaling pathways, two potential targets of 6BIO, have been reported to be involved in the regulation of endosome-lysosome trafficking. GSK-3, due to its regulation of the insulin response and of the Wnt/ β -catenin and Hedgehog pathways, has also been implicated in the biogenesis of endosomes and lysosomes.⁵⁷ Thus, it is possible that the 6BIO stimulation of ASO activity occurs at the level of the late endosome, where ASOs appear to penetrate the endosomal membrane.^{16,33} In fact, the small-molecule GSK-3 inhibitor CHIR99021 also increased SSO activity in HeLa-EGFP-654 cells (Figure 7A). Via the use of small molecules identified in similar high-throughput screens,^{17,58,59} it has previously been observed that the silencing ability of ASOs and hydrophobically modified siRNAs can be augmented through effective release from the late endosome. However, at the present time it remains an open question as to precisely how 6BIO augments ASO activity.

Our examination of AR expression in LNCaP and LAPC-4 cells subsequent to GSK-3 α and GSK-3 β silencing after siRNA treatment clearly demonstrated that 6BIO regulated AR expression through inhibition of both GSK-3 α and GSK-3 β activity. This is because three siRNAs of differing sequence, targeting the GSK-3 α and GSK-3 β mRNAs simultaneously, recapitulated the effect of 6BIO treatment

with respect to the silencing of AR mRNA and protein expression (Figure 8). However, the direct effect of siRNA-mediated GSK-3 α and GSK-3 β downregulation on oligo function could not be assessed unambiguously because the transfection step itself resulted in increased gene silencing by gymnosin, regardless of the siRNA used. We have previously observed this phenomenon, which in this case depends on increased ASO uptake and targeting ability (data not shown). Nevertheless, another GSK-3 α/β inhibitor, the small molecule CHIR99021, also improves gene silencing by gymnosin, an observation that further suggests a role for these kinases in ASO function.

The knockdown of either of the GSK-3 isoforms alone had little effect on AR silencing. This indicates a functional redundancy of GSK-3 α and GSK-3 β in the regulation of AR signaling, although these isoforms may differ with respect to other functions.⁴⁷ Congruent with our results, recent studies have also implicated GSK-3 α/β inhibition in the downregulation of AR signaling.^{60–62} Silencing of both GSK-3 α and GSK-3 β has also been demonstrated to produce a significant reduction in AR transcript levels, in addition to influencing AR stability and AR cellular localization.⁶¹ Conversely, the AR can be phosphorylated by ectopically expressed GSK-3 β or by purified GSK-3 β in vitro.⁶² GSK-3 α and GSK-3 β are also aberrantly expressed in many human prostate cancer cells.^{46,60}

Several GSK-3 inhibitors have been shown to repress AR signaling. These small molecular compounds include SB216763,⁶¹ lithium chloride (LiCl),⁶³ CHIR99021,⁴⁶ and TDZD-8.⁶³ We compared the potency of 6BIO with CHIR99021 and LiCl, and found that 6BIO is more potent on a molar basis than these other two inhibitors with respect to AR silencing (Figures 7C and 7D). We also demonstrated, for the first time to our knowledge, that GSK-3 inhibition by 6BIO

could effectively deplete AR-V7 protein levels in prostate cancer cells (Figures 6C, 6F, and 6I).

In conclusion, in this study we have demonstrated that the kinase inhibitor 6BIO not only facilitates numerous oligo activities in cells, but also represses AR expression in prostate cancer cells via inhibition of both GSK-3 α and GSK-3 β . The finding that 6BIO effectively down-regulates the expression of the AR-V7 in prostate cancer cells underlies its potential as a single agent in managing advanced prostate cancer. In contrast with the oral hormonal agents abiraterone or enzalutamide, which either block the synthesis of androgen or prevent it from binding to the AR, 6BIO promotes a reduction of AR and AR-V7 expression and reduces levels of their transcripts through inhibiting GSK-3 α and GSK-3 β activity. When combined with a therapeutic AR-ASO, this effect is even more striking. These results provide the basis for a novel anti-AR strategy.

MATERIALS AND METHODS

Cell Culture

HCT116-EGFP-miR21,²⁷ HT1080, and HeLa-EGFP-654 cells were cultured in DMEM media supplemented with 10% fetal bovine serum (FBS). The prostate cancer cell lines LNCaP, 22Rv1, and LAPC-4 were maintained in RPMI 1640 supplemented with 10% FBS. Prior to treatment the media was replaced with RPMI supplemented with 10% charcoal-dextran stripped FBS (Gemini). To facilitate cell growth, we cultured LAPC-4 cells on dishes or plates coated with PBS containing 0.01% poly-lysine (Sigma-Aldrich).

Forty microliters of cell suspension containing 20,000 HCT116-EGFP-miR21 cells was slowly pipetted into each well of a 96-well hanging drop culture plate (Perfecta3D 96-well Hanging Drop Plates; 3D Biomatrix) to create three-dimensional (3D) hanging drop cell cultures. The next day, the hanging spheres were treated by adding 10 μ L culture media containing 5 μ M miR21-ASO and 5 μ M 6BIO. Three days later, the spheres were transferred into glass-bottom plates for confocal analyses of the fluorescence signal with a two-photon confocal microscope (Zeiss Upright LSM510).

For 3D clonal cultures in Matrigel (Corning), cells were harvested as a single-cell suspension at a concentration of 1,500 cells per 50 μ L media. Matrigel was thawed at 4°C. Cold Matrigel was mixed with an equal volume of a single-cell suspension. One hundred microliters of the cold cell mixture (1,500 cells in 50% Matrigel) was pipetted around the rim of a well of a 12-well plate and then swirled so that the mixture was evenly distributed around the rim. The plate was placed into a 37°C CO₂ incubator for 30 min to allow the Matrigel to solidify. One milliliter warm complete media was added to each well without disturbing the Matrigel ring. The media was half changed every 3 days.

Oligonucleotides

In this work, all ASOs are all-PS, with DNA in small letters and LNA in capital letters. “m” represents the 5-methylcytosine modification.

The sequences of oligonucleotides used in this study are listed in Table 1.

Reagents

6BIO, CHIR99021 (CHIR), and lithium chloride (LiCl) were commercially obtained from Sigma-Aldrich. The AR antibody (N-20) was purchased from Santa Cruz Biotechnology; the GSK-3 α / β (D75D3), β -catenin (4270), and GAPDH (D16H11) antibodies from Cell Signaling Technology; the BCL2 antibody (clone 124) from Dako; and the α -Tubulin antibody from Sigma-Aldrich. The anti-GSK-3 α siRNA (6312) and the anti-GSK-3 α / β -siRNA (6301, referred as si-GSK-3 α / β -1) were purchased from Cell Signaling Technology, and the anti-GSK-3 β siRNA (s6241) from Thermo Fisher Scientific. The sequences of the other two siRNAs designed to simultaneously silence both GSK-3 α and GSK-3 β isoforms (si-GSK-3 α / β -2 or si-GSK-3 α / β 3) are proprietary.

Drug Screening

HCT116-EGFP-miR21 cells²⁷ were used in the drug screening in combination with the chemical library Tocriscreen (Tocris Bioscience). Cells were seeded into 96-well black plates with clear bottoms 1 day prior to the screening. The chemical library was dissolved in DMSO. Each compound and the miR21-ASO, both at a concentration of 1 μ M, were added to the cells for screening. All measurements were performed in duplicate. The EGFP fluorescence of HCT116-EGFP-miR21 cells was quantified with a multimode microplate reader (Tecan Infinite 200 PRO; Tecan Group).

RT-PCR

RNA was extracted from cells with RNA-STAT 60 (AMS Biotechnology) as recommended by the manufacturer. First-strand cDNAs were synthesized with the SuperScript 3 First-Strand Synthesis System kit (Invitrogen). PCR was performed with Power SYBR GREEN PCR Master Mix (Thermo Fisher Scientific). The PCR primers used in this study were as follows: full-length AR (5'-CCTGGCTTCGCAACTTACAC-3'; 5'-GGACTTGTGCATGCGGTACTCA-3'), AR-V7 (5'-CCATCTTGCTCTTCGAAATGTTA-3'; 5'-TTTGAATGAGGCAAGTCAGCCTTTCT-3'),⁶ PSA (5'-TCTGCGGCGGTGTTCTG-3'; 5'GCCGACCCAGCAAGATCA-3'), TSPRSS3 (5'-GGACAGTGTGCACCTCAAAGAC-3'; 5'-TCCCACGAGGAAGGTC CC-3'), BCL2 (5'-AAGATTGATGGGATCGTTGC-3'; 5'-GCGGAACACTTGATTCTGGT-3'), GAPDH (5'-AGGTGAAGGTCGGAGTCAAC-3'; 5'-ATCTCGCTCCTGGAAGATGG-3'), β -actin (5'-AGAAAATCTGGCACCACACC-3'; 5'-CCATCTCTTGCTCGAAGTCC-3'). In brief, PCRs were performed under optimized conditions at 95°C \times 15 s, 56°C \times 30 s, 72°C \times 30 s for 39 cycles followed by a melting curve analysis. The mRNA levels were normalized to the endogenous GAPDH or β -actin mRNA, which served as internal controls.

siRNA Transfection

LNCaP cells were seeded at 60% confluence in RPMI 1640 containing 10% FBS, 24 hr prior to transfection. Each siRNA was delivered to LAPC-4 cells, to make a final concentration of 50 nM, 4 hr

Table 1. Sequences of Oligonucleotides in This Study

Names	Sequences
Anti-miR21	5'-TcAgtCTgaTaAgCTa-3'
SSO (LNA-654)	5'-GcTaTtAcCtTaAcCc-3'
Control ASO (SPC 3046)	5'-mCGmCAGattataaAmCmCt-3'
BCL2-ASO (SPC2996)	5'-mCTcccaactgcmCmCa-3'
Cy5-ASO	5'-Cy5-mCTcccaactgcmCmCa-3'
HER3-ASO (EZN-3290)	5'-TAGcctgtcacttCTC-3'
β -Cat-ASO (EZN-3889)	5'-CCAAtcttgatCAT-3'
AR-ASO (EZN-4176)	5'-ACCaaagtcttcAGC-3'

after seeding, using Lipofectamine 3000 (Thermo Fisher Scientific) as recommended by the manufacturer. Cells were harvested 2 days following siRNA transfection for western blot and RT-PCR analyses.

Statistical Analysis

Gene expression, cell growth, number of fluorescent cells, and fluorescence intensity are represented as mean \pm SD; the statistical significance was determined by Student's t test. A p value < 0.05 was considered a statistically significant difference between the means.

SUPPLEMENTAL INFORMATION

Supplemental Information includes five figures and can be found with this article online at <http://dx.doi.org/10.1016/j.ymthe.2016.10.017>.

AUTHOR CONTRIBUTIONS

D.C. and S.N. performed the drug screening; X.Z. performed most of the experiments; D.H. provided reagents for the drug screen; X.Z., D.C., and C.S. designed the project, analyzed the data, and wrote the manuscript.

CONFLICTS OF INTEREST

The authors report no conflicts of interest.

ACKNOWLEDGMENTS

We are very grateful to Ryszard Kole and Rudolph Juliano for providing the HeLa EGFP-564 cell line, Brian Armstrong for his assistance with the microscopy, Lucy Brown and Shaun Hsueh for their assistance with the flow cytometry, Troels Koch and Bo Hansen of Roche for providing LNA oligos, and Yixian Zhang and Lee Greenberger for also providing several oligos. Research reported in this publication included work performed in the Flow Cytometry, Microscopy, and High Throughput Screening Core Facilities supported by the National Cancer Institute of the National Institutes of Health under award P30CA033572. The content is solely the responsibility of the authors and does not necessarily represent the official views of the National Institutes of Health.

REFERENCES

- Haas, G.P., Delongchamps, N., Brawley, O.W., Wang, C.Y., and de la Roza, G. (2008). The worldwide epidemiology of prostate cancer: perspectives from autopsy studies. *Can. J. Urol.* 15, 3866–3871.
- Sternberg, C.N., Petrylak, D.P., Madan, R.A., and Parker, C. (2014). Progress in the treatment of advanced prostate cancer. *Am. Soc. Clin. Oncol. Educ. Book*, 117–131.
- Tran, C., Ouk, S., Clegg, N.J., Chen, Y., Watson, P.A., Arora, V., Wongvipat, J., Smith-Jones, P.M., Yoo, D., Kwon, A., et al. (2009). Development of a second-generation antiandrogen for treatment of advanced prostate cancer. *Science* 324, 787–790.
- Attard, G., Reid, A.H., Yap, T.A., Raynaud, F., Dowsett, M., Settatree, S., Barrett, M., Parker, C., Martins, V., Folkard, E., et al. (2008). Phase I clinical trial of a selective inhibitor of CYP17, abiraterone acetate, confirms that castration-resistant prostate cancer commonly remains hormone driven. *J. Clin. Oncol.* 26, 4563–4571.
- Stein, C.A. (2015). Treatment sequencing in metastatic castration-resistant prostate cancer: a clinical commentary. *Clin. Genitourin. Cancer* 13, 407–409.
- Antonarakis, E.S., Lu, C., Wang, H., Lubner, B., Nakazawa, M., Roeser, J.C., Chen, Y., Mohammad, T.A., Chen, Y., Fedor, H.L., et al. (2014). AR-V7 and resistance to enzalutamide and abiraterone in prostate cancer. *N. Engl. J. Med.* 371, 1028–1038.
- Lu, J., Van der Steen, T., and Tindall, D.J. (2015). Are androgen receptor variants a substitute for the full-length receptor? *Nat. Rev. Urol.* 12, 137–144.
- Castanotto, D., and Stein, C.A. (2014). Antisense oligonucleotides in cancer. *Curr. Opin. Oncol.* 26, 584–589.
- Stein, C.A., and Goel, S. (2011). Therapeutic oligonucleotides: the road not taken. *Clin. Cancer Res.* 17, 6369–6372.
- Kurreck, J. (2003). Antisense technologies. Improvement through novel chemical modifications. *Eur. J. Biochem.* 270, 1628–1644.
- Wahlestedt, C., Salmi, P., Good, L., Kela, J., Johnsson, T., Hökfelt, T., Broberger, C., Porreca, F., Lai, J., Ren, K., et al. (2000). Potent and nontoxic antisense oligonucleotides containing locked nucleic acids. *Proc. Natl. Acad. Sci. USA* 97, 5633–5638.
- Juliano, R.L., and Carver, K. (2015). Cellular uptake and intracellular trafficking of oligonucleotides. *Adv. Drug Deliv. Rev.* 87, 35–45.
- Souleimanian, N., Delevey, G.F., Soifer, H., Wang, S., Tiemann, K., Damha, M.J., and Stein, C.A. (2012). Antisense 2'-deoxy, 2'-fluoroarabino nucleic acids (2'F-ANAs) oligonucleotides: in vitro gymnotic silencers of gene expression whose potency is enhanced by fatty acids. *Mol. Ther. Nucleic Acids* 1, e43.
- Soifer, H.S., Koch, T., Lai, J., Hansen, B., Hoeg, A., Oerum, H., and Stein, C.A. (2012). Silencing of gene expression by gymnotic delivery of antisense oligonucleotides. *Methods Mol. Biol.* 815, 333–346.
- Stein, C.A., Hansen, J.B., Lai, J., Wu, S., Voskresenskiy, A., Hög, A., Worm, J., Hedtjarn, M., Souleimanian, N., Miller, P., et al. (2010). Efficient gene silencing by delivery of locked nucleic acid antisense oligonucleotides, unassisted by transfection reagents. *Nucleic Acids Res.* 38, e3.
- Castanotto, D., Lin, M., Kowolik, C., Koch, T., Hansen, B.R., Oerum, H., and Stein, C.A. (2016). Protein kinase C- α is a critical protein for antisense oligonucleotide-mediated silencing in mammalian cells. *Mol. Ther.* 24, 1117–1125.
- Yang, B., Ming, X., Cao, C., Laing, B., Yuan, A., Porter, M.A., Hull-Ryde, E.A., Maddry, J., Suto, M., Janzen, W.P., and Juliano, R.L. (2015). High-throughput screening identifies small molecules that enhance the pharmacological effects of oligonucleotides. *Nucleic Acids Res.* 43, 1987–1996.
- Yamamoto, Y., Lorient, Y., Beraldi, E., Zhang, F., Wyatt, A.W., Al Nakouzi, N., Mo, F., Zhou, T., Kim, Y., Monia, B.P., et al. (2015). Generation 2.5 antisense oligonucleotides targeting the androgen receptor and its splice variants suppress enzalutamide-resistant prostate cancer cell growth. *Clin. Cancer Res.* 21, 1675–1687.
- Zhang, Y., Castaneda, S., Dumble, M., Wang, M., Mileski, M., Qu, Z., Kim, S., Shi, V., Kraft, P., Gao, Y., et al. (2011). Reduced expression of the androgen receptor by third generation of antisense shows antitumor activity in models of prostate cancer. *Mol. Cancer Ther.* 10, 2309–2319.
- Bianchini, D., Omlin, A., Pezaro, C., Lorente, D., Ferraldeschi, R., Mukherji, D., Crespo, M., Figueiredo, I., Miranda, S., Riisnaes, R., et al. (2013). First-in-human Phase I study of EZN-4176, a locked nucleic acid antisense oligonucleotide to exon

- 4 of the androgen receptor mRNA in patients with castration-resistant prostate cancer. *Br. J. Cancer* 109, 2579–2586.
21. Xiao, Z., Hao, Y., Liu, B., and Qian, L. (2002). Indirubin and meisoindigo in the treatment of chronic myelogenous leukemia in China. *Leuk. Lymphoma* 43, 1763–1768.
 22. Liu, L., Nam, S., Tian, Y., Yang, F., Wu, J., Wang, Y., Scuto, A., Polychronopoulos, P., Magiatis, P., Skaltsounis, L., and Jove, R. (2011). 6-Bromoindirubin-3'-oxime inhibits JAK/STAT3 signaling and induces apoptosis of human melanoma cells. *Cancer Res.* 71, 3972–3979.
 23. Nam, S., Buettner, R., Turkson, J., Kim, D., Cheng, J.Q., Muehlbeyer, S., Hippe, F., Vatter, S., Merz, K.H., Eisenbrand, G., and Jove, R. (2005). Indirubin derivatives inhibit Stat3 signaling and induce apoptosis in human cancer cells. *Proc. Natl. Acad. Sci. USA* 102, 5998–6003.
 24. Braig, S., Bischoff, F., Abhari, B.A., Meijer, L., Fulda, S., Skaltsounis, L., and Vollmar, A.M. (2014). The pleiotropic profile of the indirubin derivative 6BIO overcomes TRAIL resistance in cancer. *Biochem. Pharmacol.* 91, 157–167.
 25. Chebel, A., Kagiialis-Girard, S., Catalo, R., Chien, W.W., Mialou, V., Domenech, C., Badiou, C., Tigaud, I., and Ffrench, M. (2009). Indirubin derivatives inhibit malignant lymphoid cell proliferation. *Leuk. Lymphoma* 50, 2049–2060.
 26. Braig, S., Kressirer, C.A., Liebl, J., Bischoff, F., Zahler, S., Meijer, L., and Vollmar, A.M. (2013). Indirubin derivative 6BIO suppresses metastasis. *Cancer Res.* 73, 6004–6012.
 27. Castanotto, D., Sakurai, K., Lingeman, R., Li, H., Shively, L., Aagaard, L., Soifer, H., Gatignol, A., Riggs, A., and Rossi, J.J. (2007). Combinatorial delivery of small interfering RNAs reduces RNAi efficacy by selective incorporation into RISC. *Nucleic Acids Res.* 35, 5154–5164.
 28. Song, M.S., and Rossi, J.J. (2014). The anti-miR21 antagomir, a therapeutic tool for colorectal cancer, has a potential synergistic effect by perturbing an angiogenesis-associated miR30. *Front. Genet.* 4, 301.
 29. Scherr, M., Venturini, L., Battmer, K., Schaller-Schoenitz, M., Schaefer, D., Dallmann, I., Ganser, A., and Eder, M. (2007). Lentivirus-mediated antagomir expression for specific inhibition of miRNA function. *Nucleic Acids Res.* 35, e149.
 30. Wu, Y., Liu, F., Liu, Y., Liu, X., Ai, Z., Guo, Z., and Zhang, Y. (2015). GSK3 inhibitors CHIR99021 and 6-bromoindirubin-3'-oxime inhibit microRNA maturation in mouse embryonic stem cells. *Sci. Rep.* 5, 8666.
 31. Breslin, S., and O'Driscoll, L. (2013). Three-dimensional cell culture: the missing link in drug discovery. *Drug Discov. Today* 18, 240–249.
 32. Bennett, C.F., Chiang, M.Y., Chan, H., Shoemaker, J.E., and Mirabelli, C.K. (1992). Cationic lipids enhance cellular uptake and activity of phosphorothioate antisense oligonucleotides. *Mol. Pharmacol.* 41, 1023–1033.
 33. Castanotto, D., Lin, M., Kowolik, C., Wang, L., Ren, X.Q., Soifer, H.S., Koch, T., Hansen, B.R., Oerum, H., Armstrong, B., et al. (2015). A cytoplasmic pathway for gapmer antisense oligonucleotide-mediated gene silencing in mammalian cells. *Nucleic Acids Res.* 43, 9350–9361.
 34. Gemignani, F., Sazani, P., Morcos, P., and Kole, R. (2002). Temperature-dependent splicing of beta-globin pre-mRNA. *Nucleic Acids Res.* 30, 4592–4598.
 35. Chou, T.C., and Talalay, P. (1984). Quantitative analysis of dose-effect relationships: the combined effects of multiple drugs or enzyme inhibitors. *Adv. Enzyme Regul.* 22, 27–55.
 36. Chou, T.C. (2006). Theoretical basis, experimental design, and computerized simulation of synergism and antagonism in drug combination studies. *Pharmacol. Rev.* 58, 621–681.
 37. Wu, Y., Zhang, Y., Wang, M., Li, Q., Qu, Z., Shi, V., Kraft, P., Kim, S., Gao, Y., Pak, J., et al. (2013). Downregulation of HER3 by a novel antisense oligonucleotide, EZN-3920, improves the antitumor activity of EGFR and HER2 tyrosine kinase inhibitors in animal models. *Mol. Cancer Ther.* 12, 427–437.
 38. Zhang, Y., Qu, Z., Kim, S., Shi, V., Liao, B., Kraft, P., Bandaru, R., Wu, Y., Greenberger, L.M., and Horak, I.D. (2011). Down-modulation of cancer targets using locked nucleic acid (LNA)-based antisense oligonucleotides without transfection. *Gene Ther.* 18, 326–333.
 39. Blagodatski, A., Poteryaev, D., and Katanaev, V.L. (2014). Targeting the Wnt pathways for therapies. *Mol. Cell. Ther.* 2, 28.
 40. Vougianniopoulou, K., and Skaltsounis, A.L. (2012). From Tyrian purple to kinase modulators: naturally halogenated indirubins and synthetic analogues. *Planta Med.* 78, 1515–1528.
 41. Yost, C., Torres, M., Miller, J.R., Huang, E., Kimelman, D., and Moon, R.T. (1996). The axis-inducing activity, stability, and subcellular distribution of beta-catenin is regulated in *Xenopus* embryos by glycogen synthase kinase 3. *Genes Dev.* 10, 1443–1454.
 42. Cao, H., Chu, Y., Lv, X., Qiu, P., Liu, C., Zhang, H., Li, D., Peng, S., Dou, Z., and Hua, J. (2012). GSK3 inhibitor-BIO regulates proliferation of immortalized pancreatic mesenchymal stem cells (iPMSCs). *PLoS ONE* 7, e31502.
 43. Polychronopoulos, P., Magiatis, P., Skaltsounis, A.L., Myrianthopoulos, V., Mikros, E., Tarricone, A., Musacchio, A., Roe, S.M., Pearl, L., Leost, M., et al. (2004). Structural basis for the synthesis of indirubins as potent and selective inhibitors of glycogen synthase kinase-3 and cyclin-dependent kinases. *J. Med. Chem.* 47, 935–946.
 44. Hoessel, R., Leclerc, S., Endicott, J.A., Nobel, M.E., Lawrie, A., Tunnah, P., Leost, M., Damiens, E., Marie, D., Marko, D., et al. (1999). Indirubin, the active constituent of a Chinese antileukaemia medicine, inhibits cyclin-dependent kinases. *Nat. Cell Biol.* 1, 60–67.
 45. Meijer, L., Skaltsounis, A.L., Magiatis, P., Polychronopoulos, P., Knockaert, M., Leost, M., Ryan, X.P., Vonica, C.A., Brivanlou, A., Dajani, R., et al. (2003). GSK-3-selective inhibitors derived from Tyrian purple indirubins. *Chem. Biol.* 10, 1255–1266.
 46. Darrington, R.S., Campa, V.M., Walker, M.M., Bengoa-Vergniory, N., Gorrono-Etxebarria, I., Uysal-Onganer, P., Kawano, Y., Waxman, J., and Kypta, R.M. (2012). Distinct expression and activity of GSK-3 α and GSK-3 β in prostate cancer. *Int. J. Cancer* 131, E872–E883.
 47. Doble, B.W., and Woodgett, J.R. (2003). GSK-3: tricks of the trade for a multi-tasking kinase. *J. Cell Sci.* 116, 1175–1186.
 48. Ming, X., Carver, K., Fisher, M., Noel, R., Cintrat, J.C., Gillet, D., Barbier, J., Cao, C., Bauman, J., and Juliano, R.L. (2013). The small molecule Retro-1 enhances the pharmacological actions of antisense and splice switching oligonucleotides. *Nucleic Acids Res.* 41, 3673–3687.
 49. Shin, E.K., and Kim, J.K. (2012). Indirubin derivative E804 inhibits angiogenesis. *BMC Cancer* 12, 164.
 50. Blažević, T., Heiss, E.H., Atanasov, A.G., Breuss, J.M., Dirsch, V.M., and Uhrin, P. (2015). Indirubin and indirubin derivatives for counteracting proliferative diseases. *Evid. Based Complement. Alternat. Med.* 2015, 654098.
 51. Tseng, A.S., Engel, F.B., and Keating, M.T. (2006). The GSK-3 inhibitor BIO promotes proliferation in mammalian cardiomyocytes. *Chem. Biol.* 13, 957–963.
 52. Sato, N., Meijer, L., Skaltsounis, L., Greengard, P., and Brivanlou, A.H. (2004). Maintenance of pluripotency in human and mouse embryonic stem cells through activation of Wnt signaling by a pharmacological GSK-3-specific inhibitor. *Nat. Med.* 10, 55–63.
 53. Gavilán, E., Sánchez-Aguayo, I., Daza, P., and Ruano, D. (2013). GSK-3 β signaling determines autophagy activation in the breast tumor cell line MCF7 and inclusion formation in the non-tumor cell line MCF10A in response to proteasome inhibition. *Cell Death Dis.* 4, e572.
 54. Robinson, J.W., Leshchynska, I., Farghaian, H., Hughes, W.E., Sytnyk, V., Neely, G.G., and Cole, A.R. (2014). PI4KII α phosphorylation by GSK3 directs vesicular trafficking to lysosomes. *Biochem. J.* 464, 145–156.
 55. Catz, S.D., and Johnson, J.L. (2001). Transcriptional regulation of bcl-2 by nuclear factor kappa B and its significance in prostate cancer. *Oncogene* 20, 7342–7351.
 56. Campa, V.M., Baltziskueta, E., Bengoa-Vergniory, N., Gorrono-Etxebarria, I., Wesolowski, R., Waxman, J., and Kypta, R.M. (2014). A screen for transcription factor targets of glycogen synthase kinase-3 highlights an inverse correlation of NF κ B and androgen receptor signaling in prostate cancer. *Oncotarget* 5, 8173–8187.
 57. Pálffy, M., Reményi, A., and Korcsmáros, T. (2012). Endosomal crosstalk: meeting points for signaling pathways. *Trends Cell Biol.* 22, 447–456.
 58. Gilleron, J., Paramasivam, P., Zeigerer, A., Querbes, W., Marsico, G., Andree, C., Seifert, S., Amaya, P., Stöter, M., Koteliensky, V., et al. (2015). Identification of siRNA delivery enhancers by a chemical library screen. *Nucleic Acids Res.* 43, 7984–8001.

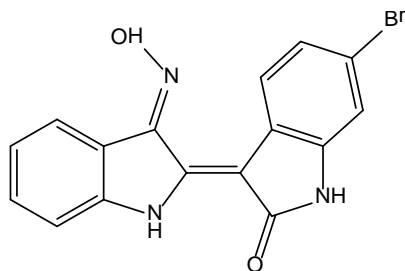
59. Osborn, M.F., Alterman, J.F., Nikan, M., Cao, H., Didiot, M.C., Hassler, M.R., Coles, A.H., and Khvorova, A. (2015). Guanabenz (Wytensin™) selectively enhances uptake and efficacy of hydrophobically modified siRNAs. *Nucleic Acids Res.* *43*, 8664–8672.
60. Li, R., Erdamar, S., Dai, H., Sayeeduddin, M., Frolov, A., Wheeler, T.M., and Ayala, G.E. (2009). Cytoplasmic accumulation of glycogen synthase kinase-3beta is associated with aggressive clinicopathological features in human prostate cancer. *Anticancer Res.* *29*, 2077–2081.
61. Rinnab, L., Schütz, S.V., Diesch, J., Schmid, E., Küfer, R., Hautmann, R.E., Spindler, K.D., and Cronauer, M.V. (2008). Inhibition of glycogen synthase kinase-3 in androgen-responsive prostate cancer cell lines: are GSK inhibitors therapeutically useful? *Neoplasia* *10*, 624–634.
62. Salas, T.R., Kim, J., Vakar-Lopez, F., Sabichi, A.L., Troncoso, P., Jenster, G., Kikuchi, A., Chen, S.Y., Shemshedini, L., Suraokar, M., et al. (2004). Glycogen synthase kinase-3 beta is involved in the phosphorylation and suppression of androgen receptor activity. *J. Biol. Chem.* *279*, 19191–19200.
63. Zhu, Q., Yang, J., Han, S., Liu, J., Holzbeierlein, J., Thrasher, J.B., and Li, B. (2011). Suppression of glycogen synthase kinase 3 activity reduces tumor growth of prostate cancer in vivo. *Prostate* *71*, 835–845.

YMTHE, Volume 25

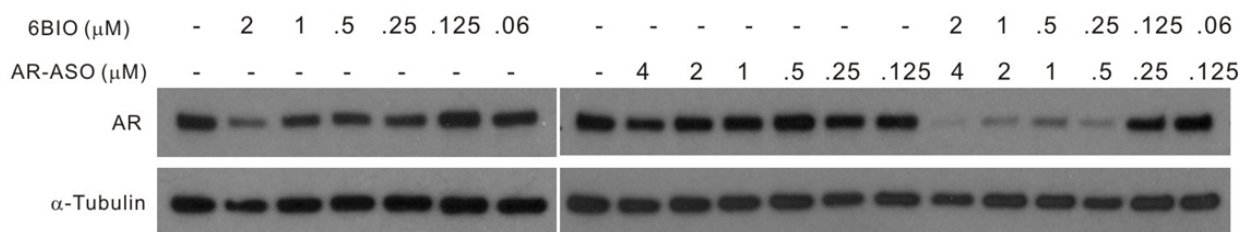
Supplemental Information

6BIO Enhances Oligonucleotide Activity in Cells: A Potential Combinatorial Anti-androgen Receptor Therapy in Prostate Cancer Cells

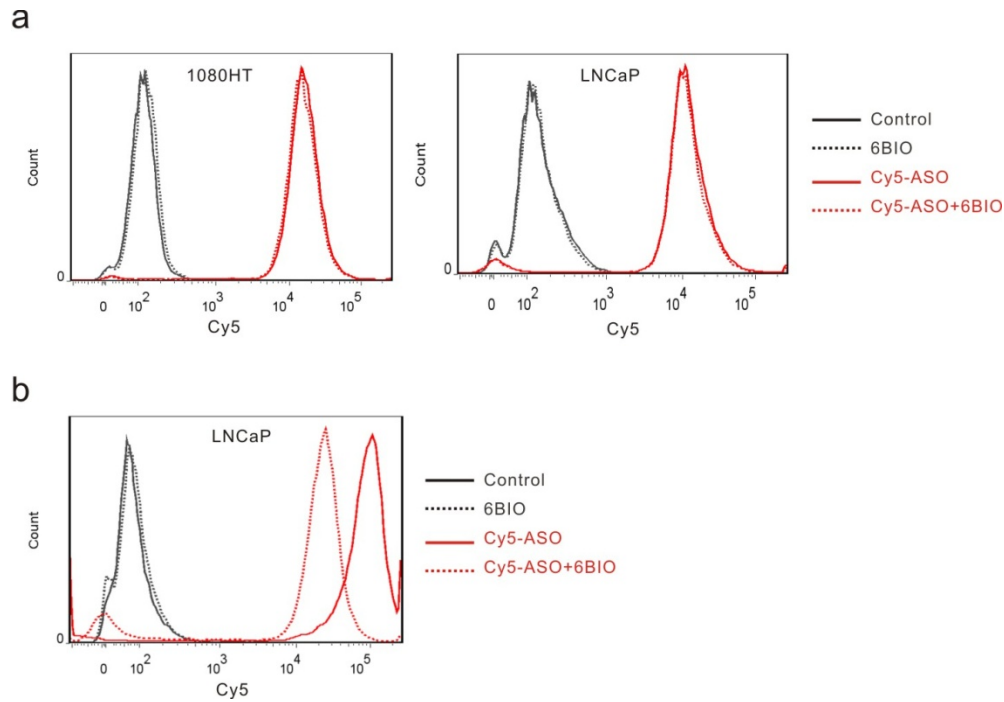
Xiaowei Zhang, Daniela Castanotto, Sangkil Nam, David Horne, and Cy Stein



Supplementary Figure S1. The molecular structure of 6BIO. 6-Bromo-indirubin-3'-oxime; its molecular formula is C₁₆H₁₀BrN₃O₂.

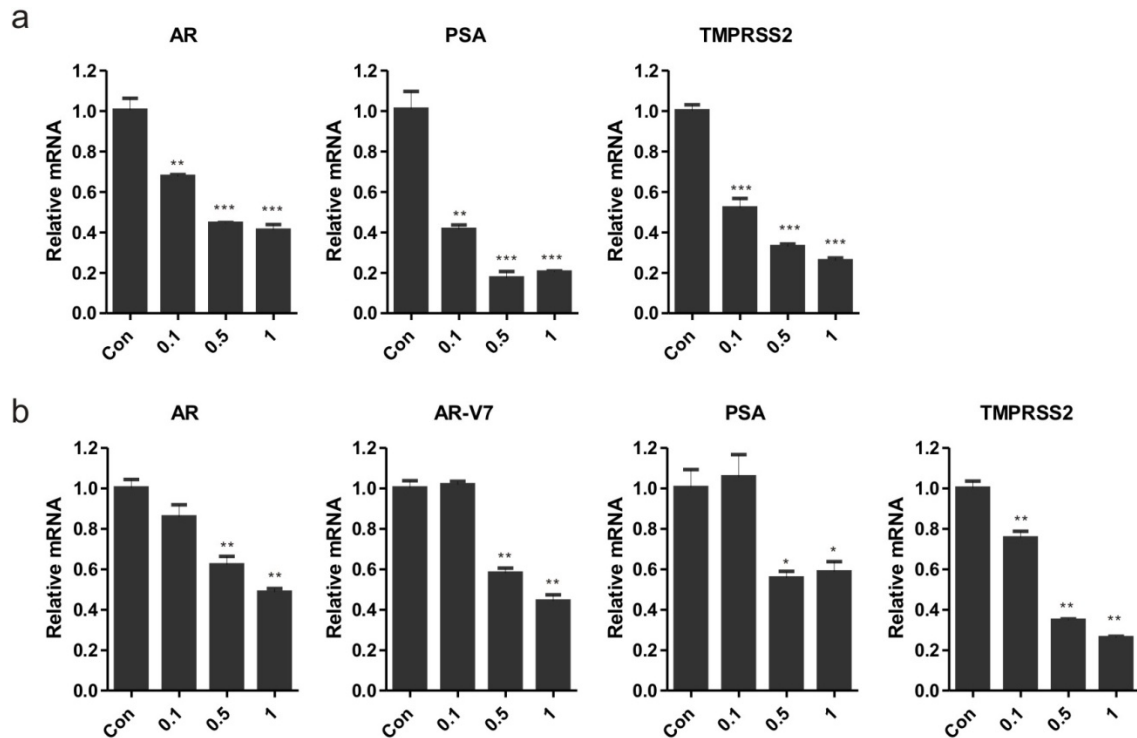


Supplementary Figure S2. Fixed concentration ratios of AR-ASO and 6BIO demonstrate synergistic AR suppression. Representative Western analysis of lysates harvested from LNCaP cells treated with increasing or decreasing concentrations of 6BIO and AR-ASO, as indicated. Three biological replicates demonstrated analogous results. Values of protein reduction for all Westerns were calculated with Image J and normalized to the α-Tubulin as the loading control and to the control, untreated cells. The values were used for the determination of the CI by the Chou-Talalay method [35]; the resulting graph is shown in Figure 5e.

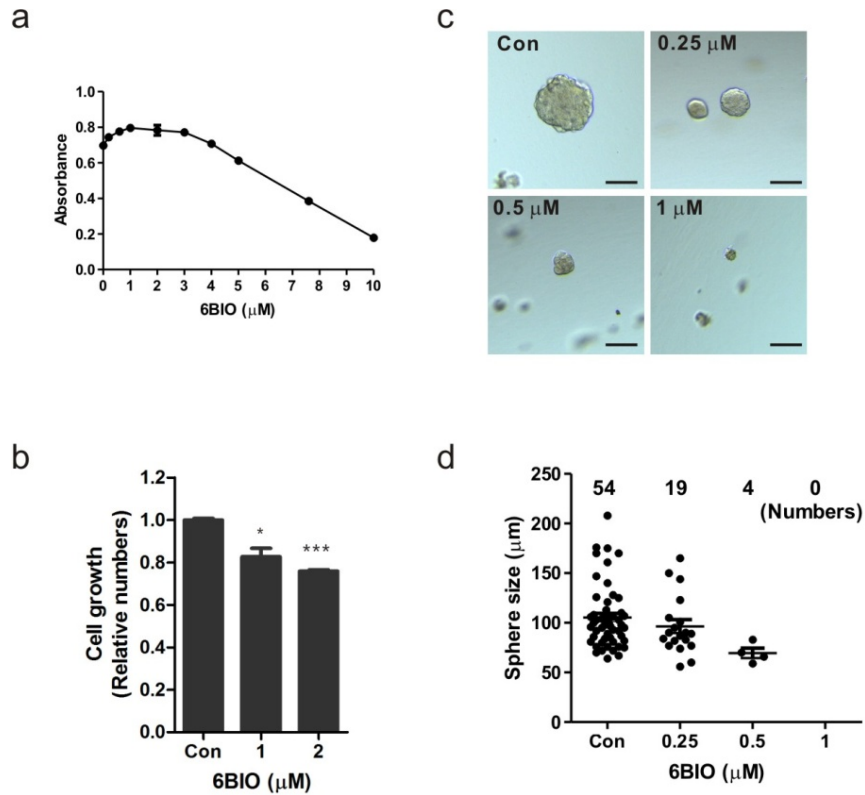


Supplementary Figure S3 6BIO does not enhance the cellular uptake of Cy5-labeled PS LNA gap-mers.

(a) A Cy5-labeled PS LNA gap-mer (Cy5-ASO) with or without 1 μ M 6BIO was delivered at 200 nM final concentration by gymnosis to HT1080 or LNCaP cells for 3 hr prior to flow cytometry. Non-treated cells were used as the control. **(b)** The identical experiment as in **a** was extended for 12 hrs in LNCaP cells prior to flow cytometry. Prolonged treatment (12 hrs) with 1 μ M 6BIO reduced the uptake of Cy5-ASO in LNCaP cells relative to the non-treated control.



Supplementary Figure S4. 6BIO represses AR mRNA expression and inhibits AR signaling in prostate cancer cells in a dose-dependent manner. Determination of AR, PSA, TMPRSS2 and AR-V7 relative expression by RT-PCR of total RNA derived from **(a)** LNCaP cells and **(b)** 22Rv1 cells, treated with increasing concentrations of 6BIO for 24 hours. Values were normalized to β -actin mRNA expression and expressed as the mean \pm s.d., $n = 3$. Student's *t*-test: *, $p < 0.05$; **, $p < 0.01$, ***, $p < 0.001$. The experiments were repeated two times with similar results.



Supplementary Figure S5. 6BIO inhibits LNCaP cell growth. **(a)** MTS assay of LNCaP cells treated with increasing concentrations of 6BIO. Data were expressed as the mean \pm s.d., $n = 3$. **(b)** Relative number of LNCaP cells established by cell counting with a hemocytometer. 700,000 LNCaP cells were cultured in 60-mm dishes and treated with 1 or 2 μM 6BIO for three days. Untreated cells served as the control for this experiment. Values were normalized to the control number and expressed as the mean \pm s.d., $n = 3$. Student's t -test: *, $p < 0.05$; ***, $p < 0.001$. **(c)** Representative growth of LNCaP microspheres in Matrigel after treatment for 12 days with the indicated increasing concentrations of 6BIO. **(d)** Tumor microsphere numbers (x-axis) and sizes (y-axis) following the 6BIO treatment as indicated in **c**. A tumor microsphere was defined as a colony with a diameter greater than 50 μM . Scale bar, 100 μM .